NASA TECHNICAL NOTE

NASA TN D-3916

NASA TN D-3916

BALLISTIC LIMIT OF DOUBLE-WALLED METEOROID BUMPER SYSTEMS

by Richard Madden

Langley Research Center

Langley Station, Hampton, Va.

NATIONAL AERONAUTICS AND SPACE ADMINISTRATION • WASHINGTON, D. C. • APRIL 1967

NASA TN D-3916

BALLISTIC LIMIT OF DOUBLE-WALLED METEOROID BUMPER SYSTEMS

By Richard Madden

Langley Research Center
Langley Station, Hampton, Va.

NATIONAL AERONAUTICS AND SPACE ADMINISTRATION

For sale by the Clearinghouse for Federal Scientific and Technical Information
Springfield, Virginia 22151 – CFSTI price $3.00

BALLISTIC LIMIT OF DOUBLE-WALLED METEOROID BUMPER SYSTEMS

By Richard Madden
Langley Research Center

SUMMARY

A model has been developed for the theoretical analysis of double-walled meteoroid bumper systems. The model is applicable for the range of velocities attributed to meteoroids in space. A normal density function has been used to represent the mass of the spray emanating from the bumper. The equations of linear plate theory are used to describe the behavior of the spacecraft main wall and to determine a ballistic limit criterion. A parametric study is performed to determine the effects of pertinent parameters. In addition, the analysis is applied to the determination of the mass distribution between bumper and main spacecraft wall that results in the greatest ballistic limit velocity for the system. The model has yielded a simple ballistic limit equation that may be used by designers of spacecraft. The equation illustrates that the ballistic limit velocity is proportional to the square of the spacing between walls and also that the highest ballistic limit velocity is achieved when the mass per unit area of the bumper equals the mass per unit area of the main wall. The theory has predicted the same trends evidenced in the highest velocity experimental data available in the literature.

INTRODUCTION

Because of the long durations of proposed space flights, the spacecraft designer must consider the structural implications of many aspects of the space environment. Of particular importance is the development of protective measures to insure the integrity of a spacecraft hull during its encounter with the meteoroid environment.

The design of protective systems depends on the ability to predict the behavior of the systems under hypervelocity impact conditions. Available theoretical analyses have yielded data on the ballistic limits of single homogeneous spacecraft walls. However, ground-facility experimentation has shown that double-walled structures or "meteoroid bumpers," illustrated in figure 1, give more meteoroid protection per unit mass than single walls. Since the information obtained from single-wall analyses is not directly applicable to double-walled structures, several authors have attempted to develop theories which describe double-wall behavior (refs. 1 and 2). In references 1 and 2 the bumper

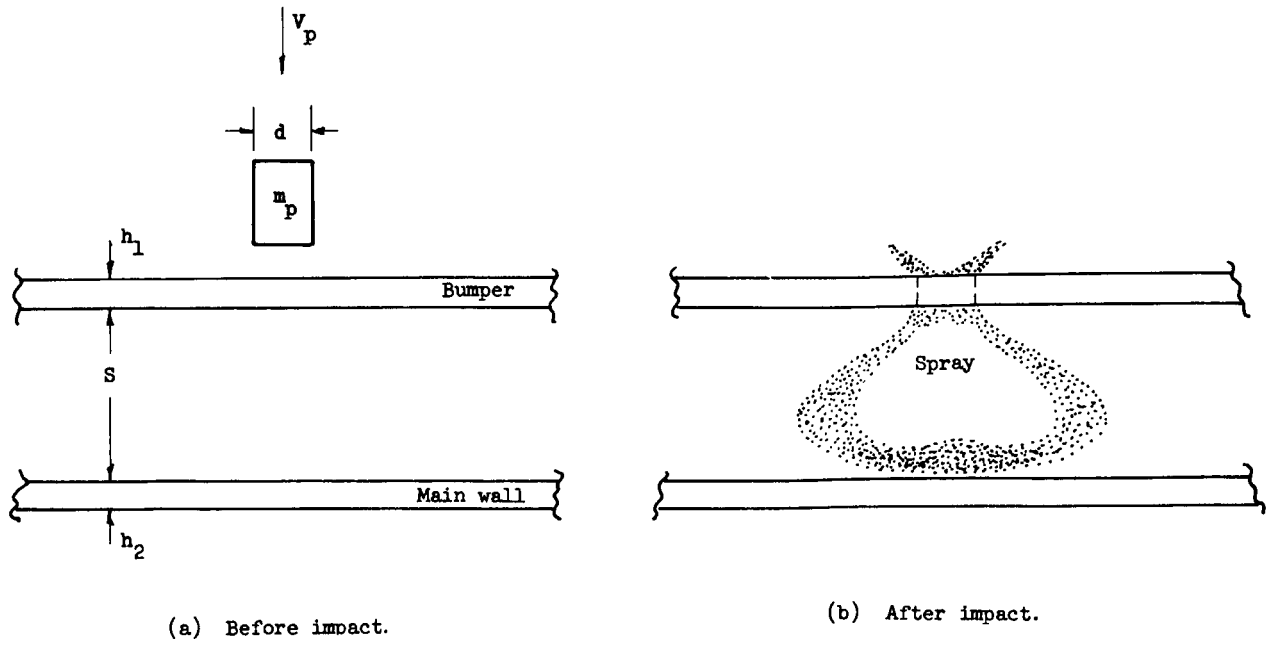

(a) Before impact. (b) After impact.

Figure 1.- Double-walled configuration before and after impact.

and main wall were treated separately. The present model was developed to integrate the behavior of the bumper and main wall so that a single expression might be available to aid the spacecraft designer in his attempt to develop adequate protective systems.

SYMBOLS

A,B constants of integration

a maximum amplitude of assumed spray-mass distribution

c speed of sound in main wall, $\sqrt{\frac{E}{\rho_2}}$

d projectile diameter

E Young's modulus of main-wall material

h_1,h_2 thickness of bumper and main wall, respectively

$J_0(pr),J_1(pr)$ Bessel functions of order 0 and 1, respectively

$K = \frac{2}{ch_2}\sqrt{3(1 - \mu^2)}$

L energy loss during impact with bumper

m_1, m_2 mass per unit area of bumper and main wall, respectively

m_* mass of bumper that contributes to spray

m_p mass of projectile

$m(r), m(\phi)$ functions describing mass distribution in spray

n integer

p transform parameter

r radial coordinate

S spacing between bumper and main wall

t time

V initial velocity of main wall

V_2 velocity imparted to main wall by spray

V_p projectile velocity

$V_{S,A}$ axial velocity of center of mass of spray

$V_{S,R}$ average radial velocity of spray

w lateral deflection of main wall

α time parameter

γ nondimensional parameter, $\dfrac{m_p(m_p + m_*)}{4m_* m_2 S^2}$

Δ standard deviation of spray-mass distribution

δt time required for spray center of mass to traverse distance between bumper and main wall

ϵ critical strain

μ	Poisson's ratio for main wall
ρ_1,ρ_2	density of bumper and main wall, respectively
σ	stress at origin
σ_{cr}	critical stress
ϕ	dummy integration variable
∇^4	biharmonic operator

A bar over a symbol indicates the forward Hankel transform of that variable.

ANALYSIS

Laboratory experiments have shown that the combined thickness of bumper and main spacecraft wall required to defeat a given projectile is not a monotonic function of velocity. In fact, three ranges are required to define the entire velocity spectrum. These ranges can be defined physically by considering the changes in phenomena which occur during and after perforation of the bumper.

Figure 2 presents the total thickness required to defeat a given projectile as a function of projectile velocity. No scale is shown, and the curve serves mainly to illustrate the trends. In the lowest velocity range the projectile remains essentially intact during perforation of the bumper and the linear relation between total thickness and velocity as derived from single-plate theory appears to be reasonable. (See, for example, ref. 3.) As the velocity increases, fragmentation of the projectile increases and consequently the slope of the curve diminishes. With further fragmentation, the curve reaches a maximum at which the low velocity range is terminated.

With further increases in velocity the intermediate range is encountered. In this range the total thickness required decreases because of the increased fragmentation and the more predominant role played by melting and vaporization in the spray. This range is terminated at a minimum which occurs when no further fragmentation and melting take place in the spray.

Additional increments in the velocity result in no phenomenological changes but do increase the impulse applied to the main spacecraft wall. The increased impulse causes greater stresses in the main wall and consequently the total thickness required to defeat the projectile again rises. This high velocity range is applicable for meteoroids.

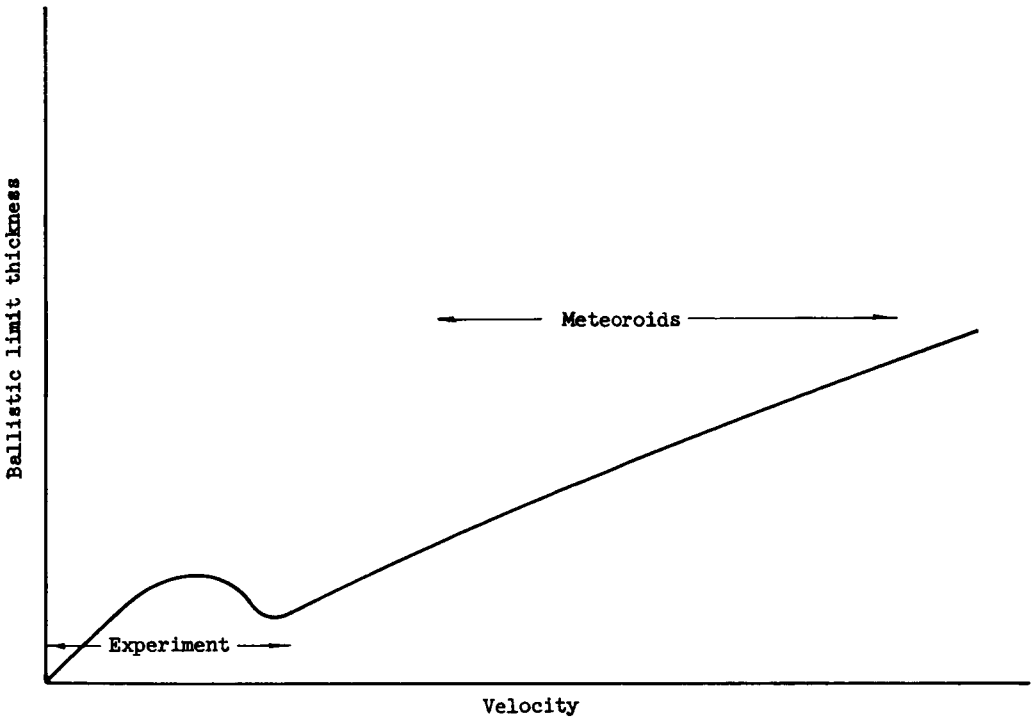

Figure 2.- Ballistic limit thickness of double-walled structures.

As illustrated in figure 2, the majority of experimental data available in the literature has been confined to the low and intermediate velocity ranges. In fact, the only available data definitely in the high velocity range are presented in reference 4.

The model developed in this paper assumes the spray to be completely fragmented and it is therefore valid only in the high velocity range. Thus, the comparison of the results from the model with experiment must be made with care to insure that the experimental data lie in the proper velocity range. The mathematical development of the model and the assumptions used in the development are discussed in the next section.

MODEL

The model is confined to the determination of the ballistic limit of the double-walled structure, and it yields no additional information on such results as hole size because linear elastic small-deflection plate theory has been used in calculations referring to the main wall. Linear plate theory, although not valid for hole-size determinations, should be valid in determining the ballistic limit, inasmuch as extremely high

strain rates develop. The stress at the axis of symmetry has been used as an indicator of the first fracture.

Assumptions

It has been assumed that the bumper serves to fragment the projectile through melting and vaporization and to diverge the spray. Momentum is conserved during impact with the bumper in order to relate the axial velocity of the center of mass of the spray to the original impact velocity. This procedure yields the familiar result, that the most important bumper property is its mass per unit area (see, for example, ref. 5).

A balance of energy for the process of impact with the bumper reveals that a portion of the original kinetic energy must be dissipated. The dissipation of this kinetic energy is the key to the present model. It is possible to dissipate this energy in many ways – for example, internal-energy increase, impact flash, or kinetic energy due to radial motion. In the present model, impact flash and internal-energy increase are assumed negligible; thus, energy is dissipated solely by radial motion of the spray. The average radial velocity of all particles is determined by equating the kinetic energy of radial velocity to the energy that must be dissipated during the impact with the bumper. It has been assumed that the spray has a uniform axial velocity as predicted from the momentum equation and therefore all particles impact the main wall at the same time. Thus all the particles are assumed to be concentrated in a plane through the center of mass perpendicular to the axial direction. This assumption is reasonable, since the velocity of the main wall after impact is much less than the velocity of the incident spray.

A Gaussian distribution of particle spray mass was assumed. This distribution approximates that found experimentally in reference 6. Also, in reference 7 it was noted that the spray-mass distribution, obtained theoretically by using a digital computer to solve the hydrodynamic equations, is approximately Gaussian.

Mathematical Development

Lateral-deflection equation.- The main wall of the spacecraft is assumed to behave elastically and the appropriate equations are taken from linear plate theory. In cylindrical coordinates the lateral-deflection equation may be written as

$$\nabla^4 w = -K^2 \frac{\partial^2 w}{\partial t^2} \tag{1}$$

where

$$\nabla^4 = \left[\frac{1}{r}\frac{\partial}{\partial r}\left(r\frac{\partial}{\partial r}\right)\right]\left[\frac{1}{r}\frac{\partial}{\partial r}\left(r\frac{\partial}{\partial r}\right)\right]$$

Since the main wall is assumed to be of infinite extent, this equation is ideally suited for a Hankel transform in the variable r (see, for example, ref. 8). The forward and inverse Hankel transforms are defined by the following integrals:

$$\bar{f}(p) = \int_0^\infty f(r) r J_0(pr) dr \tag{2}$$

$$f(r) = \int_0^\infty \bar{f}(p) r J_0(pr) dp \tag{3}$$

By multiplying equation (1) by $rJ_0(pr)dr$, integrating by parts, and then recognizing the forward transform (eq. (2)), the following equation is obtained:

$$\left\{ J_0(pr) r \frac{\partial}{\partial r}\left[\frac{1}{r}\frac{\partial}{\partial r}\left(r\frac{\partial w}{\partial r}\right)\right]\right\}_0^\infty + p\left[\frac{\partial}{\partial r}\left(r\frac{\partial w}{\partial r}\right) J_1(pr)\right]_0^\infty - p^2\left[r\frac{\partial w}{\partial r} J_0(pr)\right]_0^\infty$$

$$- p^3\left[wrJ_1(pr)\right]_0^\infty + K^2\frac{d^2\bar{w}}{dt^2} + p^4\bar{w} = 0$$

The transformed differential equation is

$$\frac{d^2\bar{w}}{dt^2} + \frac{p^4}{K^2}\bar{w} = 0 \tag{4}$$

when at the boundaries of the plate at zero and infinity

$$J_0(pr) r \frac{\partial}{\partial r}\left[\frac{1}{r}\frac{\partial}{\partial r}\left(r\frac{\partial w}{\partial r}\right)\right] = 0 \tag{5a}$$

$$\frac{\partial}{\partial r}\left(r\frac{\partial w}{\partial r}\right) J_1(pr) = 0 \tag{5b}$$

$$r\frac{\partial w}{\partial r} J_0(pr) = 0 \tag{5c}$$

$$wrJ_1(pr) = 0 \tag{5d}$$

The main wall under consideration is assumed to have zero deflection and shear per unit length at infinity and to have zero slope and finite shear at the origin. These boundary conditions, coupled with the kernel of the transform, satisfy equations (5). The solution for equation (4) may be written as

$$\bar{w} = A(p)\sin p^2\frac{t}{K} + B(p)\cos p^2\frac{t}{K}$$

Applying the condition that the initial displacement of the plate vanishes gives

$$\overline{w} = A(p)\sin p^2 \frac{t}{K} \tag{6}$$

The coefficient $A(p)$ in equation (6) is determined from the transform of initial velocity V and may be written as

$$A(p) = \frac{K}{p^2}\overline{V}(p) \tag{7}$$

Inserting equations (6) and (7) into the inverse Hankel transform (eq. (3)) gives

$$w(r,t) = K\int_0^\infty \frac{\overline{V}(p)}{p} J_0(pr)\sin p^2 \frac{t}{K}\, dp \tag{8}$$

Velocity distribution.- In analyzing a meteoroid bumper system there is no well established method for obtaining the velocity distribution applied to the spacecraft main wall. However, an approximate velocity distribution subject to an assumption on the distribution of mass in the spray emanating from the bumper may be obtained in the following manner.

The axial velocity of the center of mass of the spray is obtained by balancing the momentum of the incoming projectile and the momentum of the material forming the spray. The momentum balance is written as

$$(m_p + m_*)V_{S,A} = m_p V_p \tag{9}$$

where m_* is the mass removed from the bumper. An assumption on the value of m_* is presented subsequently.

When an energy balance is attempted, the kinetic energy after impact is found to be less than the original projectile kinetic energy. This energy must therefore be converted into internal energy, kinetic energy of radial velocity, impact flash, and so forth.

The energy equation may be written as

$$\frac{1}{2} m_p V_p^2 = \frac{1}{2}(m_p + m_*)V_{S,A}^2 + L \tag{10}$$

where L is the kinetic energy loss during the original impact. Solving for L from equations (9) and (10) gives

$$L = \frac{1}{2}\left(\frac{m_p m_*}{m_p + m_*}\right)V_p^2 \tag{11}$$

It has been assumed that all of this available energy goes into kinetic energy due to the radial velocity of the spray. Equating L in equation (11) to the kinetic energy of radial

velocity gives the average radial velocity of the spray as

$$V_{S,R} = \frac{\sqrt{m_p m_*}}{m_p + m_*} V_p \tag{12}$$

Assumed mass distribution.- As mentioned previously, the mass distribution is assumed to be approximated by a normal distribution law. The mass per unit area impacting the main wall is thus given by

$$m(r) = ae^{-\frac{1}{2}\left(\frac{r}{\Delta}\right)^2} \tag{13}$$

The two parameters a and Δ in equation (13) are determined by integrating the assumed mass distribution and equating this result to the mass of the spray and by determining the average radial location of the spray particles. By integrating the mass distribution and equating the result to the mass of the spray, the following equation is obtained:

$$m_p + m_* = 2\pi \int_0^\infty rm(r)dr \tag{14}$$

The average radial location of the spray particles is determined by multiplying the radial velocity from equation (12) by the time required for the spray to traverse the distance between the bumper and the main spacecraft wall. This time is determined from the axial velocity of the center of mass of the spray and the distance between the walls. The time is thus given by

$$\delta t = \frac{S\left(m_p + m_*\right)}{m_p V_p} \tag{15}$$

By multiplying the radial velocity by this time and equating the product to the average location of the spray particles, the following equation is obtained:

$$S\sqrt{\frac{m_*}{m_p}} = \frac{2\pi}{m_p + m_*} \int_0^\infty r^2 m(r)dr \tag{16}$$

Using equation (13) with equations (14) and (16) gives the parameters associated with the spray as

$$\left.\begin{aligned} \Delta &= S\sqrt{\frac{2m_*}{\pi m_p}} \\ a &= \left(\frac{m_p + m_*}{4S^2}\right)\left(\frac{m_p}{m_*}\right) \end{aligned}\right\} \tag{17}$$

Balancing the momentum of the spray from the bumper before impact with the main wall, and the momentum of the spray and main spacecraft wall after impact, gives

$$2\pi \int_0^r \phi m(\phi) \frac{m_p V_p}{m_p + m_*} d\phi = 2\pi \int_0^r \left[m(\phi) + m_2\right] V_2 \phi \, d\phi$$

where $m_2 = \rho_2 h_2$. By substituting the assumed mass distribution from equation (13) and equating integrands, the velocity distribution applied to the main wall may be written as

$$V_2 = \frac{m_p V_p}{\left(m_p + m_*\right) + 4m_2 S^2 \frac{m_*}{m_p} e^{\frac{1}{2}\left(\frac{r}{\Delta}\right)^2}} \tag{18}$$

where Δ is determined from equations (17).

Stresses and ballistic limit equation.- A critical stress at the origin is used as the criterion for the ballistic limit. At the origin the radial and circumferential stresses are equal; therefore either stress may be considered. From linear plate theory the appropriate equation is

$$\sigma = - \frac{Eh_2}{2(1 - \mu)} \left(\frac{\partial^2 w}{\partial r^2} \right)_{r=0} \tag{19}$$

It should be noted that at the origin, since both stresses are equal, the critical-stress criterion is equivalent to a critical-strain criterion. The relation between stress and strain is

$$\sigma = \frac{E}{1 - \mu} \epsilon \tag{20}$$

Equation (8) may now be differentiated twice with respect to r, evaluated at $r = 0$, and substituted into equation (19) to yield

$$\sigma = \frac{KEh_2}{4(1 - \mu)} \int_0^\infty p \bar{V}(p) \sin p^2 \frac{t}{K} \, dp \tag{21}$$

The integral representation of the transformed initial velocity (obtained by applying equation (2) to equation (18)) is inserted into equation (21) and the resulting equation is reduced to give

$$\frac{\sigma}{E} \frac{c}{V_p} \sqrt{\frac{1 - \mu}{3(1 + \mu)}} \left(1 + \frac{m_*}{m_p}\right) = \int_0^\infty \frac{p}{2} \int_0^\infty \frac{r J_0(pr) dr}{1 + \frac{1}{\gamma} e^{\frac{1}{2}\left(\frac{r}{\Delta}\right)^2}} \sin p^2 \frac{t}{K} \, dp \tag{22}$$

where

$$\gamma = \frac{m_p(m_p + m_*)}{4m_*m_2S^2}$$

By expanding the interior integral for values of $\gamma < 1$ and integrating term by term, the following equation is obtained:

$$\frac{\sigma}{E}\frac{c}{V_p}\sqrt{\frac{1-\mu}{3(1+\mu)}}\left(1+\frac{m_*}{m_p}\right) = \Delta^2\int_0^\infty \frac{p}{2}\sin p^2\,\frac{t}{K}\sum_{n=1}^{\infty}(-1)^{n+1}\frac{\gamma^n}{n}e^{-\frac{p^2\Delta^2}{2n}}\,dp \qquad (\gamma < 1)$$

Performing the integration yields

$$\frac{\sigma}{E}\frac{c}{V_p}\sqrt{\frac{1-\mu}{3(1+\mu)}}\left(1+\frac{m_*}{m_p}\right) = \frac{1}{2}\sum_{n=1}^{\infty}(-1)^{n+1}\,n\gamma^n\,\frac{\alpha}{1+n^2\alpha^2} \qquad (\gamma < 1) \qquad (23)$$

where

$$\alpha = \frac{2}{\Delta^2}\frac{t}{K}$$

If the series is maximized in time to determine the maximum stress, α in equation (23) may be determined from

$$\sum_{n=1}^{\infty}(-1)^{n+1}n\gamma^n\frac{1-n^2\alpha^2}{\left(1+n^2\alpha^2\right)^2} = 0 \qquad (24)$$

Equations (23) and (24) may be solved to give the ballistic limit for any system with $\gamma < 1$. However, present impact tests and meteoroid experiments correspond to values of γ on the order of 0.01 or less. Thus, a one-term expansion in equations (23) and (24) is adequate to describe all practical systems. The full series solution of equations (23) and (24) is used only to determine the limits of applicability of the simplified solution (see fig. 3).

Simplified ballistic limit equation.- Performing the one-term expansion on equations (23) and (24) yields the following simplified ballistic limit equation:

$$\frac{V_p}{c} = 16\,\frac{\sigma_{cr}}{E}\sqrt{\frac{1-\mu}{3(1+\mu)}}\,\frac{S^2m_*m_2}{m_p^2} \qquad (\gamma << 1) \qquad (25)$$

It should be noted that the one-term solution corresponds physically to neglecting the mass of the spray after impact in determining the initial velocity applied to the main wall. In the present analysis m_* is taken to be the mass of a disk of the same diameter as

the original projectile. This assumption may be easily modified when experiment or theory gives a better value for m_*. Therefore,

$$m_* = \frac{\pi d^2}{4} m_1 \tag{26}$$

Inserting this expression for m_* into equation (25) gives

$$V_p = \left[4\pi \frac{\sigma_{cr}}{E} \sqrt{\frac{1 - \mu}{3(1 + \mu)}}\, c \right] \frac{S^2 d^2 m_1 m_2}{m_p^2} \qquad (\gamma << 1) \tag{27}$$

The quantity in brackets is composed of material constants for the main wall; however, a value of the critical fracture stress is not available at the required strain rates. It is suggested that the bracketed quantity be lumped into one factor which may be determined from impact experiments.

Inspection of equation (27) reveals that the ballistic limit velocity is linearly proportional to the mass per unit area of the bumper, the mass per unit area of the main wall, and the square of the spacing and is inversely proportional to the square of the projectile mass. Caution must be used in determining the dependence on the projectile diameter since the projectile mass is also a function of the diameter.

Optimum mass distribution.- One of the fundamental problems in meteoroid bumper design is the determination of the distribution of mass between the bumper and main wall that yields the highest ballistic limit velocity. The symmetry in equation (27) requires that the optimum distribution be $m_1 = m_2$ or, equivalently, that the mass per unit area of the bumper equal the mass per unit area of the main wall.

RESULTS AND DISCUSSION

Results are presented for the ballistic limits and the optimum distribution of mass between bumper and main spacecraft wall for double-walled structures. These results have been obtained by using both the simplified solution and the full series expansion. Representative plots have been included for the ballistic limit velocity, as a function of the double-wall parameter γ, and the variation of ballistic limit velocity with distribution of mass between bumper and main wall.

In figure 3 a nondimensional ballistic limit velocity is shown plotted as a function of γ for both the full series solution, equation (23), and the simplified solution, equation (25). The two solutions differ by approximately a factor of two in the area of $\gamma = 1$; however, for $\gamma < 0.06$ they are essentially identical. Since they behave essentially the same over the entire range of γ between 0 and 1, the trends predicted from the simplified solution are also applicable to the full series.

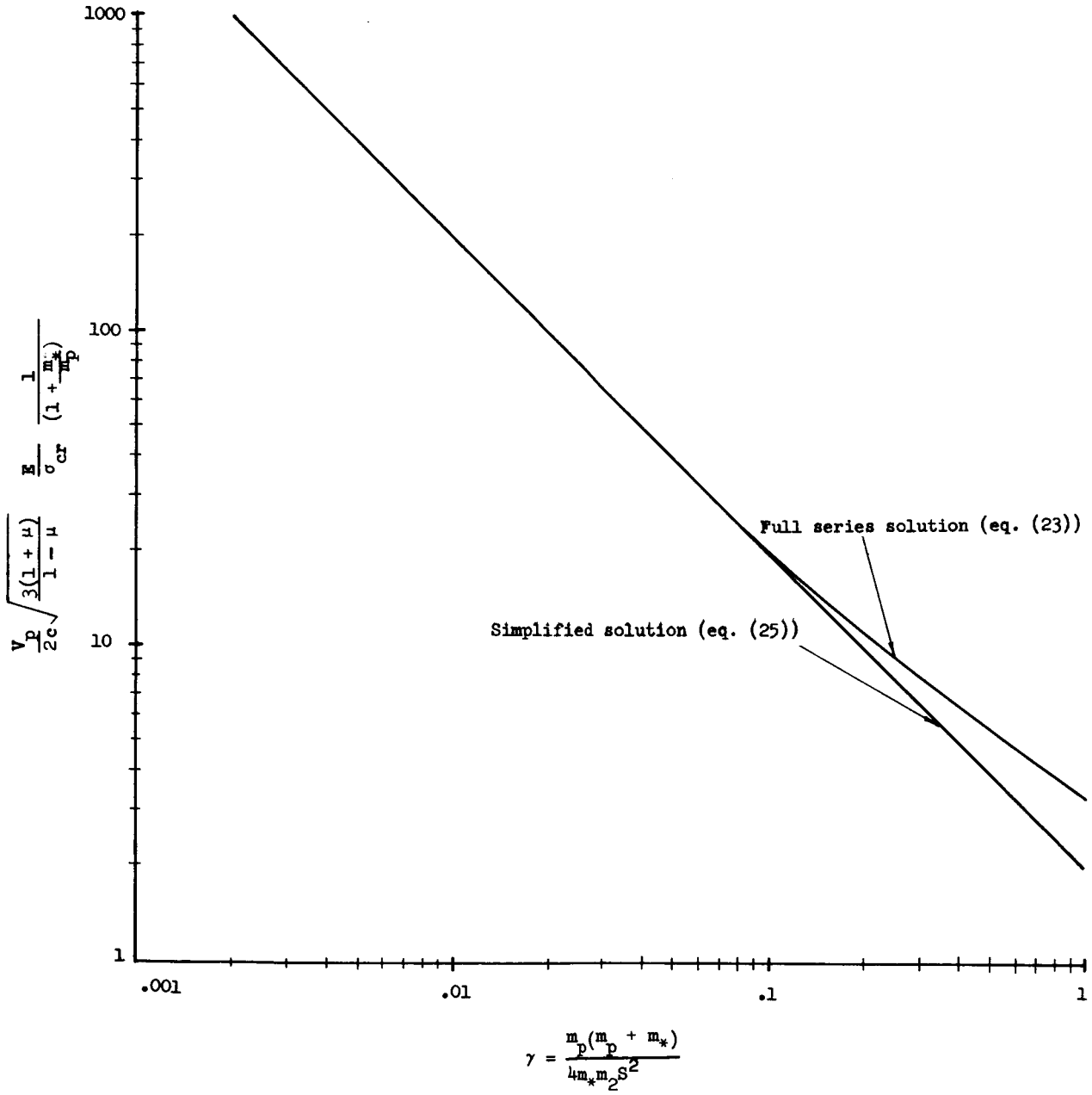

Figure 3.- Nondimensional ballistic limit velocity as a function of parameter γ.

The trends predicted from equation (25) seem to be substantiated experimentally. The linear dependence on the mass per unit area of the bumper has been observed by many experimentalists (see, for example, ref. 8). The dependence on the spacing squared and the fact that the required backup thickness is a function of the projectile diameter cubed were observed in reference 2. If a spherical or cylindrical projectile of unit aspect ratio is assumed, equation (27) predicts the backup thickness as a function of the fourth power of the projectile diameter. However, caution must be applied in trying to verify the entire formula since the equation is valid only in the highest velocity regime. Only recently have data been obtained at velocities high enough to constitute compatability with this theory (see ref. 4). Unfortunately the high-velocity data are not sufficiently refined for use in giving concrete data points to validate the theory. However, they can be and have been used to evaluate trends.

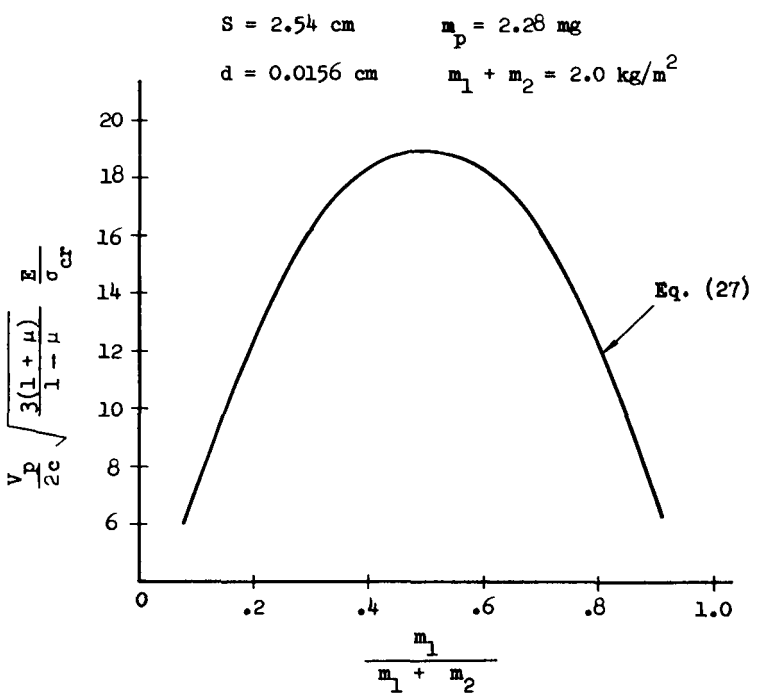

Figure 4.- Nondimensional ballistic limit velocity as a function of distribution of mass between bumper and main wall.

Figure 4 illustrates the behavior of a nondimensional ballistic limit velocity as the mass distribution between the bumper and main wall is varied. The curve is symmetrical about the maximum, where the mass per unit area is equally apportioned. The curve illustrates the same tendency as the reduced data in reference 4 – that is, a parabolic distribution with a maximum when the mass per unit area of the bumper and main wall are equal. Early experimental results have indicated that the system with 25 percent of the mass per unit area allotted to the bumper is the most efficient. This result is plausible for the low and intermediate velocity ranges since the spray is not completely fragmented. However, for the high velocity range, where the spray is entirely fragmented, the present result is applicable, as evidenced by recent experimentation (ref. 4).

CONCLUDING REMARKS

The methods of linear plate theory have been used to develop an expression for the ballistic limit of double-walled structures. This expression predicts behavior which corresponds to the highest velocity experiments available in that it predicts that the ballistic limit is a linear function of the mass per unit area of the bumper and a quadratic function of the spacing between the walls. The optimum distribution of mass between the bumper and main wall also coincides with experimental findings at high velocities.

The model is not expected to correlate with experiment in the velocity ranges at which data are usually collected (the low and intermediate ranges). Therefore, in any attempt at verifying the model or using the results, it must be assured that the system is operating in the high velocity range. The expected velocities for hazardous meteoroids will surely be within the high velocity range. The model should give some insight into the relation of parameters in the determination of ballistic limits for double-walled systems.

Langley Research Center,
National Aeronautics and Space Administration,
Langley Station, Hampton, Va., December 8, 1966,
124-08-01-13-23.

REFERENCES

1. Johnston, Reed H.; Knapton, David A.; and Lull, David: Meteoroid Bumper Protection for Space Vehicles – Tentative Design Criteria. Rept. No. 65008-05-01 (Contract No. NASw-615), Arthur D. Little, Inc., June 1963.

2. Maiden, C. J.; McMillan, A. R.; Sennett, R. E.; and Gehring, J. W.: Experimental Investigations of Simulated Meteoroid Damage to Various Spacecraft Structures. TR65-48 (Contract NAS9-3081), GM Defense Res. Lab., Gen. Motors Corp., July 1965.

3. Thomson, Robert G.; and Kruszewski, E. T.: Effect of Target Material Yield Strength on Hypervelocity Perforation and Ballistic Limit. Proceedings of the Seventh Hypervelocity Impact Symposium, vol. V, Feb. 1965, pp. 273-320. (Sponsored by U.S. Army, U.S. Air Force, and U.S. Navy.)

4. Posever, F. C.; and Scully, C. N.: Investigation of Meteoroid Impacts on Two-Sheet Configurations. Tech. Rept. AFFDL-TR-65-196, U.S. Air Force, Nov. 1965.

5. Nysmith, C. Robert; and Summers, James L.: An Experimental Investigation of the Impact Resistance of Double-Sheet Structures at Velocities to 24,000 Feet Per Second. NASA TN D-1431, 1962.

6. Becker, Karl R.; Watson, Richard W.; and Gibson, Frank C.: Hypervelocity Impact Phenomena. Bur. Mines, U.S. Dept. Interior, Apr. 5, 1962.

7. Riney, T. D.; and Heyda, J. F.: Hypervelocity Impact Calculations and Their Correlation With Experiment. Tech. Inform. Ser. No. R64SD64 (Contract No. AF 08(635)-3781), Missile Space Div., Gen. Elec. Co., Sept. 1964.

8. Sneddon, Ian N.: Fourier Transforms. First ed., McGraw-Hill Book Co., Inc., 1951.

NASA-Langley, 1967 — 32 L-5318

10-5-67

"The aeronautical and space activities of the United States shall be conducted so as to contribute . . . to the expansion of human knowledge of phenomena in the atmosphere and space. The Administration shall provide for the widest practicable and appropriate dissemination of information concerning its activities and the results thereof."

—NATIONAL AERONAUTICS AND SPACE ACT OF 1958

NASA SCIENTIFIC AND TECHNICAL PUBLICATIONS

TECHNICAL REPORTS: Scientific and technical information considered important, complete, and a lasting contribution to existing knowledge.

TECHNICAL NOTES: Information less broad in scope but nevertheless of importance as a contribution to existing knowledge.

TECHNICAL MEMORANDUMS: Information receiving limited distribution because of preliminary data, security classification, or other reasons.

CONTRACTOR REPORTS: Scientific and technical information generated under a NASA contract or grant and considered an important contribution to existing knowledge.

TECHNICAL TRANSLATIONS: Information published in a foreign language considered to merit NASA distribution in English.

SPECIAL PUBLICATIONS: Information derived from or of value to NASA activities. Publications include conference proceedings, monographs, data compilations, handbooks, sourcebooks, and special bibliographies.

TECHNOLOGY UTILIZATION PUBLICATIONS: Information on technology used by NASA that may be of particular interest in commercial and other non-aerospace applications. Publications include Tech Briefs, Technology Utilization Reports and Notes, and Technology Surveys.

Details on the availability of these publications may be obtained from:

SCIENTIFIC AND TECHNICAL INFORMATION DIVISION

NATIONAL AERONAUTICS AND SPACE ADMINISTRATION

Washington, D.C. 20546